Quaternary Research 85 (2016) 25–33

Contents lists available at ScienceDirect

Quaternary Research

journal homepage: www.elsevier.com/locate/yqres

Changes in glacier extent and surface elevations in the Depuchangdake region of northwestern Tibet, China

Zhiguo Li [a,b,*], Lide Tian [b], Hongbo Wu [c], Weicai Wang [b], Shuhong Zhang [d], Jingjing Zhang [a], Xuexin Li [a]

[a] Department of Environment and Planning, Shangqiu Normal University, Shangqiu, China
[b] Institute of Tibetan Plateau Research, Chinese Academy of Sciences, Beijing, China
[c] School of History and Tourism, Shaanxi University of Technology, Shaanxi Hanzhong 723000, China
[d] Department of Life Science, Shangqiu Normal University, Shangqiu, China

ARTICLE INFO

Article history:
Received 27 March 2015
Available online 14 January 2016

Keywords:
Glacier variations
Remote sensing
Transition zone
Depuchangdake region

ABSTRACT

Remote sensing data, including those from Landsat Thematic Mapper/Enhanced Thematic Mapper Plus (TM/ETM+), the Shuttle Radar Topography Mission Digital Elevation Model (SRTM4.1 DEM), and the Geoscience Laser Altimeter System Ice, Cloud, and Land Elevation Satellite (Glas/ICESat), show that from 1991 to 2013 the glacier area in the Depuchangdake region of northwestern Tibet decreased from 409 to 393 km^2, an overall loss of 16 km^2, or 3.9% of the entire 1991 glacial area. The mean glacier-thinning rate was -0.40 ± 0.16 m equivalent height of water per year (w.e./yr), equating to a glacier mass balance of -0.16 ± 0.07 km^3 w.e./yr. Total mass loss from 2003 to 2009 was -1.13 ± 0.46 km^3. Glacier retreat likely reflects increases in annual total radiation, annual positive degree days, and maximum temperature, with concurrent increases in precipitation insufficient to replenish glacial mass loss. The rate of glacier retreat in Depuchangdake is less than that for Himalayan glaciers in Indian monsoon-dominated areas, but greater than that for Karakoram glaciers in mid-latitude westerly-dominated areas. Glacier type, climate zone, and climate change all impact on the differing degrees of long-term regional glacial change rate; however, special glacier distribution forms can sometimes lead to exceptional circumstances.

Introduction

The Tibetan Plateau and bordering mountains (TPB) contain the largest concentration of glaciers outside of the Polar Regions (Yao, 2008) and are often referred to as the world's "Third Pole." Glacial changes in the TPB can alter atmospheric circulation patterns and affect agriculture, power generation, and the water supplies of the 1.5 billion people that live in the region (Immerzeel et al., 2010; Piao et al., 2010; Qiu, 2010). In addition, rising meltwater streams and expanding areas of glacial meltwater-fed lakes caused by glacier retreat have deeply impacted local ecosystems and flooded pastures (Yao, 2010). Therefore, alongside scientific interest, understanding glacial change has important socioeconomic and political implications.

Previous research has defined the extent of glacier retreat varies across the TPB and has shown systematic differences in glacier status between Himalaya and Karakoram (Yao et al., 2012; Gardner et al., 2013). Most glaciers in the eastern, central and western Himalaya have decreased in extent since the 1970s (Ye et al., 2008; Li et al., 2011; Wang et al., 2015a), which likely reflects rising temperatures and decreasing precipitation (Yao et al., 2012; Wiltshire et al., 2014; Yang et al., 2014). Mass loss has been higher in western Himalaya than in eastern and central Himalaya (Gardelle et al., 2013). In contrast, Karakoram glaciers have remained stable or advanced over the same period (Hewitt, 2005; Kaab et al., 2012; Yao et al., 2012; Gardelle et al., 2013; Gardner et al., 2013; Neckel et al., 2014). This pattern, which was first highlighted by Hewitt (2005) and is known as the Karakoram Anomaly, and contrasts markedly with a worldwide decline in mountain glaciers. The Karakoram Anomaly is attributed to increased snowfall and cooling at high altitudes (Hewitt, 2005; Wiltshire et al., 2014; Yang et al., 2014).

The transition zone between the Himalaya and Karakoram (TZHK) is bordered to the west by Jammu–Kashmir and Himachal Pradesh, on the east by Depuchangdake, on the south by Ayilariju, and on the north by Xiongcaigangri. Glaciers in Himachal Pradesh are shrinking (Gardelle et al., 2013; Mir et al., 2014), while those in Jammu–Kashmir have decreased, increased or fragmented, or have not change in extent from 1962 to 2001, with most glaciers apparently stable from 2001 to 2009 (Ghosh et al., 2014). A 5.6% glacier area loss (6.5 km^2) occurred between 1980 and 2010 in the Shyok Basin, with small glaciers retreating and large glaciers advancing, especially during the last decade (Bajracharya et al., 2015). Ayilariju glaciers along the southern border of the TZHK are retreating comparatively rapidly (Li et al., 2015a), while the Xiongcaigangri and neighboring glaciers on the northern border of the TZHK are retreating relatively slowly (Brahmbhatt et al., 2015; Li et al.,

* Corresponding author at: Department of Environment and Planning, Shangqiu Normal University, Shangqiu, China.
E-mail address: lizhiguo999999@163.com (Z. Li).

http://dx.doi.org/10.1016/j.yqres.2015.12.005
0033-5894/

2015b). However, although glacier volume change across the region had been reported in the TPB using remote sensing data (Kääb et al., 2012; Gardelle et al., 2013; Gardner et al., 2013; Neckel et al., 2014) and field observations (Yao et al., 2012), mass change in Depuchangdake glaciers has not been reported.

Investigating glacial changes in the TZHK may help to reveal the roles and processes driving the spatial heterogeneity of glacier change, i.e., how and why glaciers change from retreating to advancing states across the TPB. Our study focused on glacier area changes from 1991 to 2013 in the Depuchangdake region of the Tibetan Plateau. In particular, glacier mass balance changes from 2003 to 2009 were identified and possible control mechanisms were considered.

Study area

The Depuchangdake region is situated on the northwestern edge of the Tibetan Plateau, east of the Karakoram, northeast of the Western Himalaya, and south of West Kunlun (Fig. 1). Asian monsoons and westerly cyclones influence the climate of the Depuchangdake region, and local glaciers have been classified as polar continental-type (Shi, 2008). Depuchangdake glaciers provide fresh water for Jiezechaka, Longmu, Woerba and Lumajiangdong lakes (Fig. 1). According to Landsat image obtained in1991, 303 glaciers lie within the study area, comprising a total area of ~409 km^2, and with a mean glacier area of ~1.35 km^2 at the time of mapping. Glacier areas for Jiezechaka, Longmu, Woerba and Lumajiangdong lakes in the Depuchangdake regions are 134, 26, 100, and 149 km^2, respectively.

The mean equilibrium-line altitude (ELA) for glaciers in the Depuchangdake region is ~5900 m above sea level (asl; Shi, 2008; Yao et al., 2012). The mean annual air temperature and precipitation from 1961 to 2013 were ~0.71°C and 70.6 mm, respectively, as measured at Shiquanhe station (a national reference climatological station at 32°30′N/80°08′E, 4279 m asl).

Data and methods

Remote sensing data

Landsat Thematic Mapper/Enhanced Thematic Mapper Plus (TM/ETM+) images were used to extract glacier extent values and to monitor glacier changes. A total of 7 images were used to interpret glacier status in 1991, 2001, and 2013 (Table 1). Cloud cover in the 1991 TM, 2001 ETM+, and 2013 ETM+ images was < 4% and did not occur over the glaciers; thus, cloud cover had little impact on the delineation of glacier outlines. In addition, 7 other images from 2002 to 2009 were used to classify glacier surface cover and determine density parameters, i.e., firn, snow, and glacier ice, which helped to calculate glacier volume changes. All of the images used for area extraction were acquired near the end of the ablation season and had nearly no cloud cover. Either one or two additional images were taken at approximately the same time to provide reference data for determining seasonal snow cover and data gaps. Landsat images were provided by the U.S. Geological Survey (USGS; http://glovis.usgs.gov) and the Global Land Cover Facility. We used manual digitization to delineate glacier boundaries, as recommended by Raup et al. (2007) beacuse this provided the best tool for extracting reliable information from satellite images.

Glaciers were separated according to ridgelines generated from the Shuttle Radar Topography Mission Digital Elevation Map (SRTM 4.1 DEM) and Google Earth. The SRTM DEM was obtained in February 2000, and this dataset contains ~80% of Earth's surface elevation data at a spatial resolution of 90 m. The SRTM 4.1, whose study area data gaps were processed by Reuter et al. (2007), was selected and obtained from the Consultative Group on International Agricultural Research-Consortium for Spatial Information (CGIAR-CSI; http://srtm.csi.cgiar.org/). The SRTM DEM was also used to yield various glacier parameters, including elevation, slope, and aspect.

Ice, Cloud, and Land Elevation Satellite (ICESat) and Global Land Surface Altimetry satellite (GLAS) data were used to examine glacier change. GLA01 (release version 33) and GLA14 (release version 34) data were downloaded from the U.S. National Snow and Ice Data Center (NSIDC; http://nsidc.org/data/icesat/data.html). A total of 768 GLAS footprints (Fig. 2) for the glaciated areas of the study region were collected between 26 February 2003 and 10 October 2009. The methods of Wang et al. (2015b) were used to correct saturation elevations caused by the slope and roughness of the ICESat products. Next, glacier surface cover classifications and density parameters, i.e., firn, snow, and glacier ice surface area, were computed on the basis of GLAS waveforms and corresponding Landsat TM/ETM images from the same year. Then, glacial mass balance in each 300-m altitudinal zone was calculated using the formula of Wang et al. (2015b):

$$b_m = \frac{1}{S_m}\left(s_{\text{snow}} \times \rho_{\text{snow}} \times \Delta\overline{h}_{\text{snow}} + s_{\text{firn}} \times \rho_{\text{firn}} \times \Delta\overline{h}_{\text{firn}} + s_{\text{ice}} \times \rho_{\text{ice}} \times \Delta\overline{h}_{\text{ice}}\right) \quad (1)$$

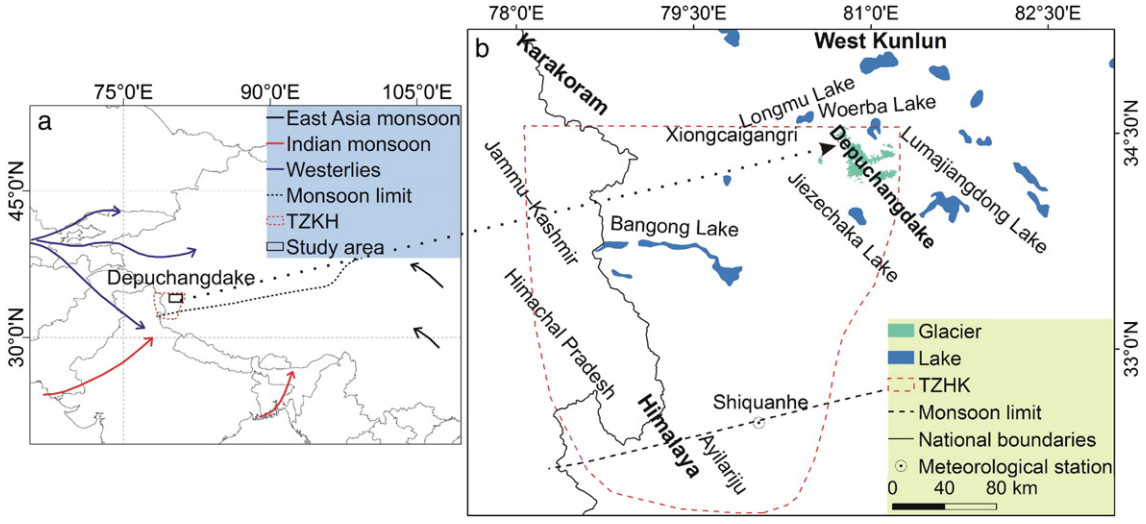

Fig. 1. Study region maps showing the distribution of glaciers and the Shiquanhe meteorological station. (a) Location of the study area within the Tibet Plateau region. Arrows denote westerly and monsoon moisture paths. The dashed line denotes the mean monsoon margin (after Chen et al., 2008), which fluctuates with season and year. (b) Overview of the study area and Shiquanhe station overlain on the digital elevation model (DEM).

https://doi.org/10.1016/j.yqres.2015.12.005 Published online by Cambridge University Press

Table 1
Landsat TM/ETM+, Landsat 8 OLI, SRTM and GLAS Data used for this study.

Data source	Acquisition date	Path, row	Image resolution (m)	Utilization	DEM error (m)
Landsat TM	17 Oct 1991	145/036	28.5	Glacier extraction	
Landsat TM	19 Aug 1993	145/036	28.5	Reference data	
Landsat ETM+	29 Sep 1999	145/036	28.5	Reference data	
Landsat ETM+	03 Jan 2000	145/036	28.5	Reference data	
Landsat ETM+	20 Oct 2001	145/036	28.5	Glacier extraction	
Landsat ETM+	02 Aug 2013	145/036	28.5	Glacier extraction	
Landsat 8 OLI	27 Sep 2013	145/036	30	Reference data	
Landsat 8 OLI	13 Sep 2014	145/036	30	Reference data	
SRTM	11 to 22 Feb 2000		90		16
GLA01, GLA14	26 Feb 2003 to 01 Dec 2008		70		0.10

where m is the *t*th altitudinal zone with intervals of 300 m, S_m are glacier areas at intervals of 300 m altitude, and ρ_{snow}, ρ_{firn}, and ρ_{ice} are and snow density (350 kg/m^3), firn density (550 kg/m^3), and glacier ice density (900 kg/m^3), respectively (Ligtenberg et al., 2011).

The regional glacier mass balance b_g was calculated according to the formula of Wang et al. (2015b):

$$b_g = \frac{1}{S}\sum_{t=1}^{m} S_m \times b_m = \frac{1}{S}\sum_{t=1}^{m}\sum_{t=1}^{n} s_i \times \rho_i \times \overline{h}_{i,m} \quad (2)$$

where S is the entire mountain glacier areas, s_i is the difference between the glacier-covered area in the altitudinal zone and the area-weighted average density, ρ_i combines ρ_{ice}, ρ_{snow}, and ρ_{firn}; t is the index of the altitudinal zone, where $t = 1, 2, 3,\ldots, m$; and i is the number of each type of glacier surface covered, where $i = 1, 2, 3,\ldots, n$.

Meteorological data

No weather stations operated within the study area during the study period, with the nearest station being located at Shiquanhe, ~200 km from Depuchangdake glaciers; however, as no high terrain obstacles exist between the meteorological station and the glacier region, the climate at Shiquanhe station is similar to that of the study area. Meteorological data from the Shiquanhe station were downloaded from the China Meteorological Data Sharing Service System (http://cdc.nmic.cn/home.do) and were used to analyze climate change. As the main ablation form for polar continental-type glaciers is sublimation caused by radiation (Zhang et al., 1996), annual total radiation was selected as the main variable, in addition to annual positive degree-days, maximum temperature, and precipitation.

Precision evaluation

The error estimation method of image co-registration mirrored the approach used by previous researchers (Ye et al., 2006; Cao et al., 2014; Wang et al., 2014). Errors extracted from multi-temporal satellite images resulted mainly from: 1) sensor resolution; 2) co-registration errors; and 3) boundary delineations. The first two error types were evaluated using a remote sensing uncertainty evaluation formula (Ye et al., 2006), with linear uncertainty expressed as:

$$U_L = \sqrt{\sum \lambda^2} + \sqrt{\sum \sigma^2} \quad (3)$$

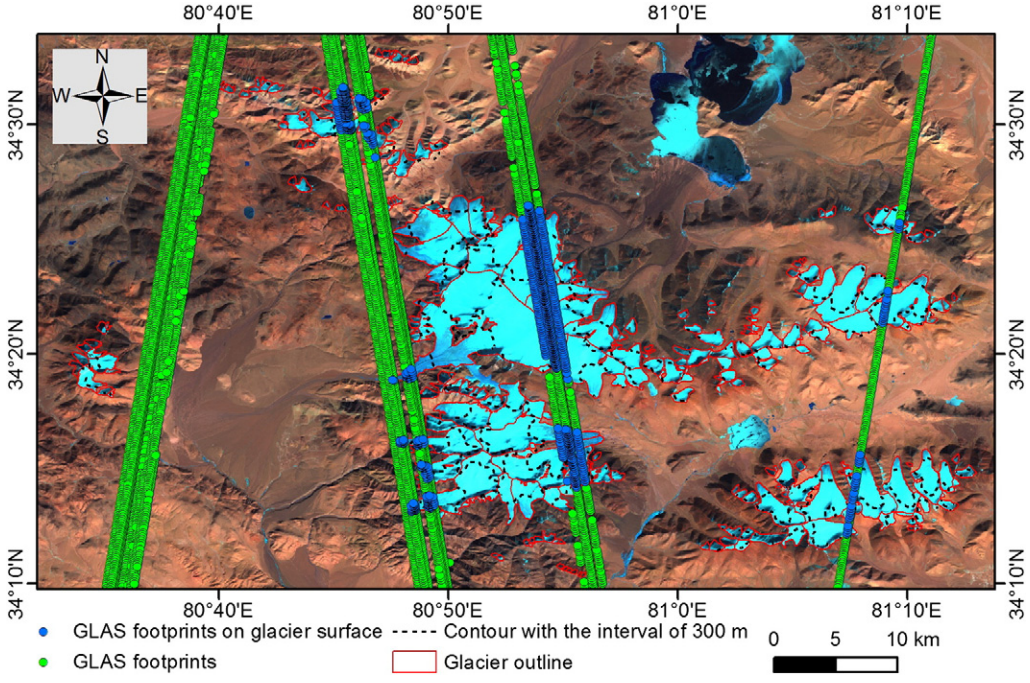

Fig. 2. Geoscience Laser Altimeter System (GLAS) footprint distributions in the Depuchangdake region. The true color image represents a combination of bands 7, 4, and 2 of the Landsat 5 satellite on 9 November 2011 (scene path 145 and row number 36 for Landsat Thematic Mapper/Enhanced Thematic Mapper Plus [TM/ETM+] Pre-WRS-2 data). Blue circles of the GLAS data are projected onto glaciated regions and green circles are projected on non-glacial regions using the WGS_1984_UTM_Zone_44N coordinate system. The distribution of interannual glacier surface area change subdivided into 300 m intervals was estimated by GLAS footprint elevation data from 2003 to 2009.

https://doi.org/10.1016/j.yqres.2015.12.005 Published online by Cambridge University Press

where U_L is the measurement uncertainty of the glacier termini in the study area, λ is the original pixel resolution of each image, and σ is the co-registration error between multiple images.

The area uncertainty between multiple remote sensing data was expressed as:

$$U_A = \sum \lambda^2 * \frac{2 * U_L}{\sqrt{\sum \lambda^2}} + \sum \sigma^2 \quad (4)$$

where U_A denotes the measurement uncertainty of the glacier area, and U_L gives the linear uncertainty. Eqs. (3) and (4) were used to calculate the uncertainty of glacier termini positions (where most of the changes occurred) and measured glacier areas (Table 2).

Glacial delineation errors resulted mainly from the experience of the operator, especially regarding the classification of shadowed areas as perennial or seasonal snow (Xiang et al., 2014). Changes in glacial area between the 1991 Landsat TM and the 2013 Landsat ETM+ images were delineated by two additional independent operators to estimate the level of error. The differences between the operators were within 3%. Tests and analyses showed that the determined differences in glacial area caused by image quality (which can be affected by seasonal snow and shadow) were <2%.

Homogeneous horizontal and vertical errors were estimated using the method of Wu et al. (2014). Homogeneous horizontal errors were 0.23 ± 6.7 m and vertical errors were from −0.08 to 0.16 m for GLAS footprint data in the study area. Glacier surface elevation differences were between −231 cm and 147 cm, with a mean value of −6.34 cm (Fig. 3a). The overall uncertainty of the GLAS footprints was from 0.16 cm to 40.26 cm, with a mean vertical error of 9.47 cm, and absolute uncertainty values that increased with slope ($y_{\text{uncertainty}} = -0.164x_{\text{slope}} + 1.1498$, $R^2 = 0.1686$; Fig. 3b).

Results and discussion

In the Depuchangdake region, parts of some glaciers are debris-mantled, mainly in front of glacier tongues. In such cases, glacial extents were not reconstructed because of the difficulties in delimiting their true extent under thick debris mantles. The distribution of Depuchangdake glaciers based on their 1991 areas and glacier area changes from 1991 to 2013 was analyzed as shown in Supplementary 1 and 2 (inlcuding data on glacier area, glacier area change and topographic features). Glacier location was shown in Supplementary 2 (Fig. S1).

Distribution of Depuchangdake glaciers: 1991

Glacier size and topographic features, e.g., elevation, slope, and aspect, varied from glacier to glacier and may have affected their rates of change. The 303 glaciers in the Depuchangdake region were classified into six groups, based on their 1991 areas. We examined the number, area, and percentage change of each group during the study period (Fig. 4a). In 1991, 235 glaciers had areas of < 1 km^2, which accounted for 77.6% of the total number of glaciers and 17.4% of the total area. Sixty-eight glaciers had areas of > 1 km^2, accounting for 22.4% of the total number of glaciers and 82.6% of the total area. Of these, 21 had areas of > 5 km^2, accounting for 7.3% of the total of number of glaciers and 57.0% of the total area.

The glacier area elevation distribution in 1991 was between 5393 and 6582 m asl, with a mean elevation of 5964 m asl. We divided the glacier area distribution into six 200-m elevation intervals, based on the SRTM DEM, and analyzed the amount of glacier area change within these elevation intervals (Fig. 4b). The results showed that glacier areas increased with elevation to a maximum at 5800–6000 m asl, above which they decreased. Most glacier areas (365.1 km^2) were within the three elevation intervals between 5600 m and 6200 m asl, which accounted for 89.3% of the total area. Glacier areas in the other three intervals covered only 43.6 km^2, accounting for just 10.7% of the total area. Glacier area distribution mainly reflects precipitation and terrain.

As a function of slope, four slope intervals between 15° and 35° contained a total of 277 glaciers, accounting for 91.4% of the total number, while the other three intervals contained 26 glaciers, accounting for 8.6% of the total number (Fig. 4c). The four intervals between 5° and 25° contained a combined glacier area of 383.7 km^2, accounting for 93.9% of the total area, while the other two intervals contained a total area of 25.1 km^2, and accounting for 4.2% of the total area.

As a function of aspect, the percentage of glaciers facing east, southeast, south, southwest, west and northwest was > 10.2% apiece, accounting for 91.7% of the total number of glaciers (Fig. 4d). The percentages of glaciers facing north and northeast were 0.7 and 7.6%, respectively. The most common aspects were east, southeast, south, southwest and west, which cumulatively accounted for 96.2% of the total glacier area.

Glacier area changes

Total glacier area in the study region decreased from 408.8 km^2 in 1991 to 393.0 km^2 in 2013, corresponding to an ice loss of 15.75 km^2 and an overall reduction of 3.9% (Table 3). The mean observed decrease in glacier area was 0.2% per year. Glacier retreat examples were shown in Fig. 5a. Eight small glaciers, which had initial areas of 0.1–0.2 km^2, disappeared between 1991 and 2013, with two disappearing during 1991–2001, and six during 2001–2013. Furthermore, one glacier with an area of 0.2 km^2 in 1991 had separated into two glaciers by 2013. The mean areal shrinkage rate showed temporal variations, with the values between 2001 and 2013 that were 2.6 times greater than those between 1991 and 2001. Large glaciers were concentrated in the central region of Depuchangdake, and these retreated less than the smaller glaciers scattered near the edges of the study area. Centrally located large glaciers may reflect a special local environment, i.e., high albedo, cold local temperatures, with reduced ablation. Glaciers on the east slope of Depuchangdake were relatively stable, with the termini of two large glaciers (No. 215 Glacier and No. 217 Glacier) retreating slightly between 1991 and 2001 (from 13.36 and 13.72 km^2 in 1991, to 13.34 and 13.69 km^2 in 2001, respectively), followed by slight termini advances between 2001 and 2013 (to 13.44 and 13.83 km^2, respectively; Fig. 5b). The loss of area mainly occurred at the glacier termini; however, some shrinkage occurred at glacier areas distributed on the mountain ridges, which became partially exposed. The glacier area changes in Jiezechaka, Woerba, Longmu and Lumajiangdong lakes in the Depuchangdake region are 3.36, 4.23, 4.95, and 3.21 km^2, respectively.

The 235 glaciers with an initial (1991) area of <1 km^2 accounted for 70.4% of the total decrease in area over the study period. The sixty-eight glaciers with initial areas of >1 km^2 accounted for 29.6% of the total decrease during the study period. Of these, 21 glaciers with initial areas of >5 km^2 accounted for 11.1% of the total decrease in area. We observed an inverse correlation between glacier size and the observed mean percentage area decrease, indicating that small glaciers receded faster (Fig. 6a). In total, 14.5 km^2 of glaciated area (91.9% of the total glacier area lost from 1991 to 2013) was located between elevations of 5393 and 6000 m asl. Glacier areas at elevations of >6250 m asl showed no change. We observed an inverse correlation between elevation gradient and observed mean percentage area decrease, indicating that glacier areas in lower elevations receded faster (Fig. 6b). Glaciers on all slopes decreased in area between 1991 and 2013 (Fig. 6c). The largest area

Table 2
Uncertainty analysis between data from different time periods.

Periods	Data	Linear uncertainty (m)	Area uncertainty (km^2)
1991–2001	Landsat TM–Landsat ETM+	45.64	0.004
2001–2013	Landsat ETM+–Landsat TM	45.64	0.004

https://doi.org/10.1016/j.yqres.2015.12.005 Published online by Cambridge University Press

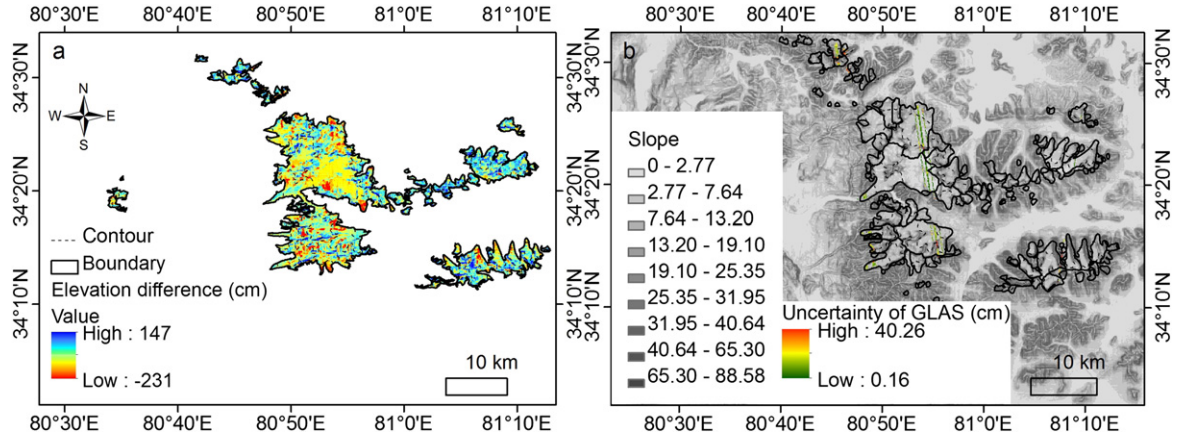

Fig. 3. Vertical errors in the Geoscience Laser Altimeter System (GLAS) footprints of Depuchangdake glaciers: (a) Distribution of elevation differences. (b) Uncertainty distribution of GLA01 data with slope.

change occurred for glaciers on slopes between 10° and 30°, where the percentage area decreases in the four slope internals were >10.2% apiece, accounting for a combined area reduction of 14.2 km^2 (or 90.4% of the total decrease). We also observed an inverse correlation between slope interval and observed mean percentage area decrease, indicating that steeper glaciers receded faster (Fig. 6d). Glaciers with all aspects retreated between 1991 and 2013; however, the largest areas of loss were for east- and southeast-facing glaciers, which accounted for 20.1 and 24.2% of the overall area loss, respectively. The largest percentage area decreases occurred for glaciers facing north, northeast, east, and northwest, which are the leeward slopes of the Indian monsoons.

Glacier mass balance changes

We observed a sustained negative mass balance and a slight negative growth trend from February 2003 to December 2009 (Fig. 7a). The vertical errors of the GLAS footprint on the glacier surface ranged from −0.08 to 0.16 m (Fig. 7b), which resulted in an underestimation of in situ measurement. Furthermore, the ice and firn dynamic imbalance, e.g., accumulation and ablation rate variations, solid precipitation, firn/snow compaction rate, glacier surging, and bedrock motion, also contributed to an underestimation of the actual bias (Wu et al., 2014). For Depuchangdake glaciers, the mean glacier thinning rate was -0.40 ± 0.16 m equivalent height of water per year (w.e. /yr), equating

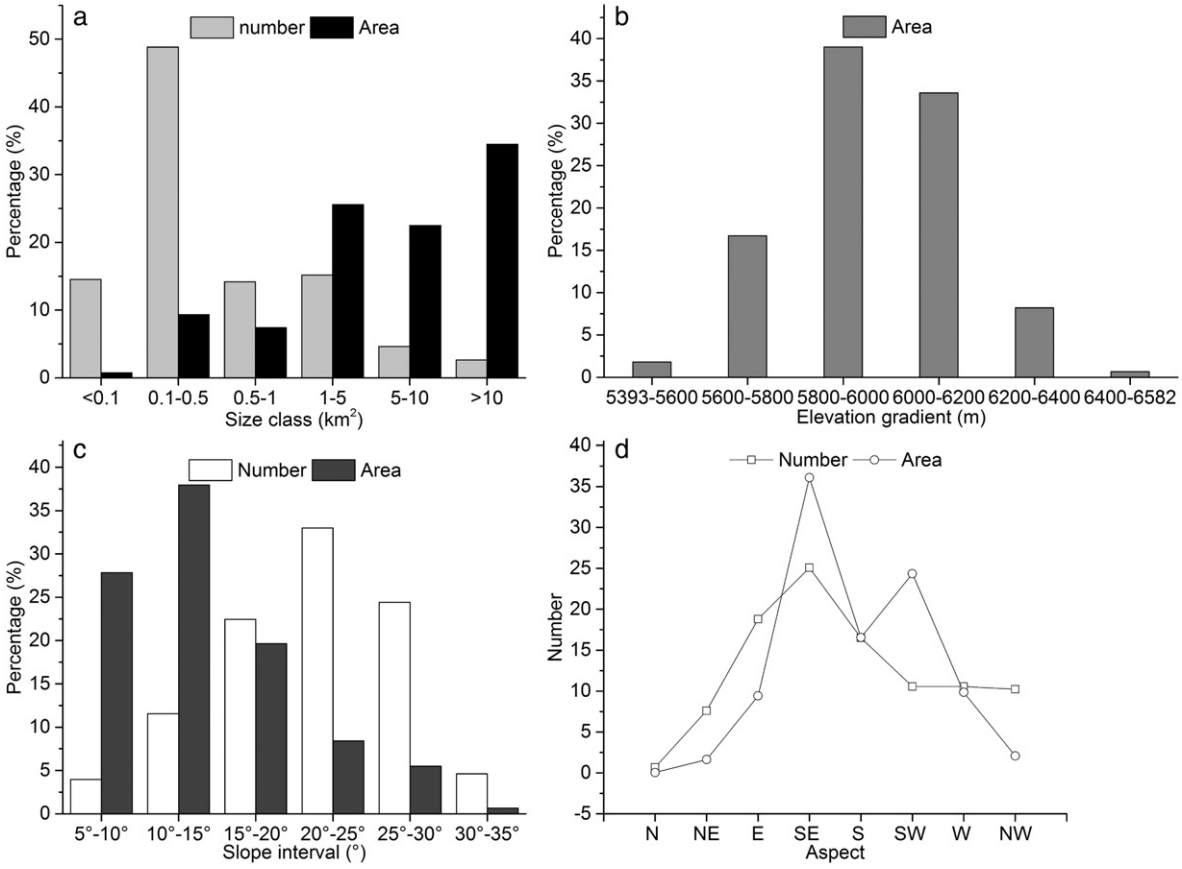

Fig. 4. Glacier characteristics in 1991. (a) Glacier number and area distribution as a function of size class. (b) Glacier area distribution as a function of elevation. (c) Glacier number and area distribution as a function of slope class. (d) Glacier number and area distribution as a function of aspect.

https://doi.org/10.1016/j.yqres.2015.12.005 Published online by Cambridge University Press

Table 3
Glacier area variations in the Depuchangdake region between 1991 and 2013.

Date	Area (km^2)	Period and area change			Relative area change	
		Period	Area change (km^2)	Mean rate (km^2/a)	Percentage (%)	Mean rate (%)
1991	408.78					
2001	404.40	1991–2001	−4.38	−0.44	−1.1	−0.1
2013	393.02	2001–2013	−11.38	−0.95	−2.8	−0.2
Total		1991–2013	−15.75	−0.72	−3.9	−0.2

to a glacier mass balance of -0.16 ± 0.07 km^3 w.e./yr. The total mass loss over the period 2003–2009 was -1.13 ± 0.46 km^3, and the glacial meltwater flow into Jiezechaka, Woerba, Longmu and Lumajiangdong lakes was 0.38 ± 0.15, 0.07 ± 0.03, 0.28 ± 0.11 and 0.41 ± 0.16 km^3, respectively.

No. 215 Glacier (34°16′N, 80°53′E) and No. 217 Glacier (34°15′N, 80°54′E) advanced between 2001 and 2013 (Fig. 5b) were different from other glaciers, glacier area distribution and glacier volume change may be the driving factor. The proportion of snow cover areas for No. 215 Glacier and No. 217 Glacier were 86.1 and 79.2% in 2001, respectively. From February 2003 to September 2003, the accumulation areas of No. 215 Glacier and No. 217 Glacier increased by 18.0 and 14.6 cm, respectively. Both glaciers are located on east-facing slopes, and their accumulation zones are associated with those of other glaciers. Snow is supplied by wind from the west (southwest monsoon or mid-latitude westerlies). Increasing precipitation since 2002 may be the cause of the glaciers' elevation increases and termini advances. Glacier type, climate zone, and climate change determine differences in long-term regional glacial retreat rate; however, as demonstrated by No. 215 Glacier and No. 217 Glacier, special glacier distribution forms sometimes lead to exceptional circumstances.

Glacier retreat and climate change

Annual total radiation, annual positive degree days, maximum temperature, and precipitation have all have increased over the past 23 years (Fig. 8). Increases in total radiation, annual positive degree days, and maximum temperature, which all reflect the regional impacts of climate change, impact on glacier mass balance, and in particular cause increased glacier ablation and promote glacier shrinkage. This trend is generally consistent with the decrease in glacier extent observed in the study area, and although precipitation showed an increasing trend, it remained insufficient to replenish glacier mass loss. The impact of these variables was confirmed by the temporal differences observed for mean annual total radiation, annual positive degree days, maximum temperature, and precipitation of 1991–2001 and 2001–2013, amounting to 333 MJ/m^2, 6.39 d, 0.90°C and −2.46 mm, respectively. The faster glacier retreat rates between 2001 and 2013 clearly corresponded to the increases in these variables.

Comparison with other regions

We compared the rates of change with those in other regions experiencing decreases in glacier cover and found that glacier area shrinkage generally decreases from the outer edge of the Himalaya (monsoon-dominated regions) toward the continental interior (mid-latitude westerly dominated regions), which is consistent with previous findings (Fig. 9; Yao et al., 2012). The Indian summer monsoons and the winter mid-latitude westerlies, both of which affect the Depuchangdake region, combine with huge topographic landforms to exert a climatic control on glacier distribution and development in the TPB (Bolch et al., 2012; Yao et al., 2012; Mölg et al., 2014). Weakening of the Indian summer monsoon and strengthening of mid-latitude westerlies (Yao et al., 2012), and the interplay of both circulation systems, has governed glacier mass balance. Glaciers of the TPB exhibit an overall shrinking trend, with the highest rates of shrinkage observed in the monsoon-influenced northeastern and southeastern margins of the plateau. In contrast, the northwestern regions are influenced more by mid-latitude westerlies and have shown balanced or advancing trends (Bolch et al., 2012; Yao et al., 2012; Gardelle et al., 2013; Gardner et al., 2013; Neckel et al., 2014). The rate of glacier retreat in Depuchangdake is less than in Indian monsoon-dominated areas, but more than in mid-latitude westerly dominated areas (where mass gains have been reported). The reduction of area for Depuchangdake glaciers is faster than that for Xiongcaigangri (Li et al., 2015a) and West Kunlun (Li et al., 2013), possibly because Depuchangdake glaciers are located near the monsoon margin. Glacier retreat rates for Depuchangdake and Ayilariju were greater than those for Xiongcaigangri and West Kunlun, possibly reflecting mean glacier size and mean elevation (Table 4), with small and lower elevation glaciers tending to retreat faster. Ayilariju lies in the monsoon-dominated region, and the speed of areal retreat at Depuchangdake exceeds that of adjoining Xiongcaigangri (in southern Karakoram) by a factor of ~15. The speed of glacier area reduction of the individual Depuchangdake glaciers may imply that Depuchangdake glaciers are somewhat affected by the Indian monsoon.

The negative glacier mass balance for the Depuchangdake region observed in this study are consistent with the results of other glacier mass balance studies in the TPB, including Gardner et al. (2013) and Neckel et al. (2014), who reported values of −0.12 to 0.16 m w.e./yr (Pamir, Karakoram, and western Kunlun) and 0.03 ± 0.25 m w.e./yr (western Kunlun and southern Karakoram), respectively. However, these differences may reflect the different methods employed. For example, in this study we used slope adjustments of GLAS footprints based on SRTM, but did not address the potential penetration of SRTM.

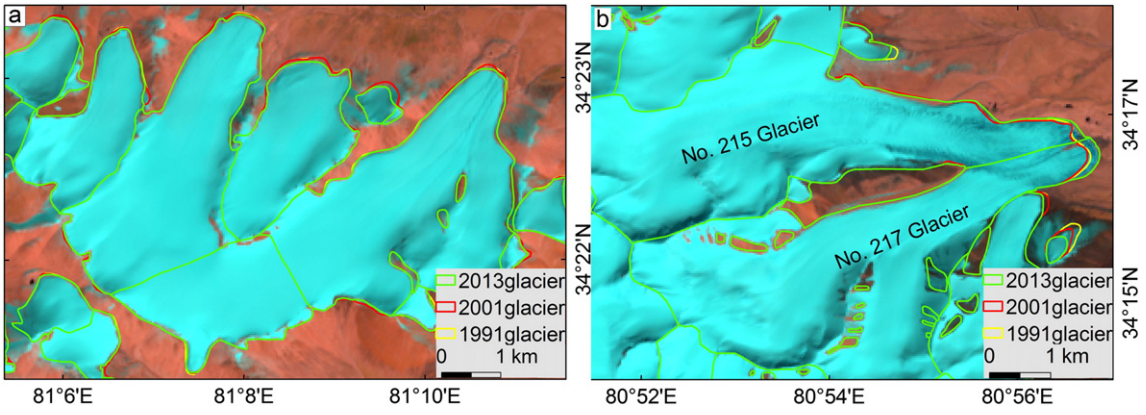

Fig. 5. Glacier changes over the study period. (a) Example of glacial retreat between 1991 and 2013. (b) Examples of two glaciers that advanced between 2001 and 2013.

https://doi.org/10.1016/j.yqres.2015.12.005 Published online by Cambridge University Press

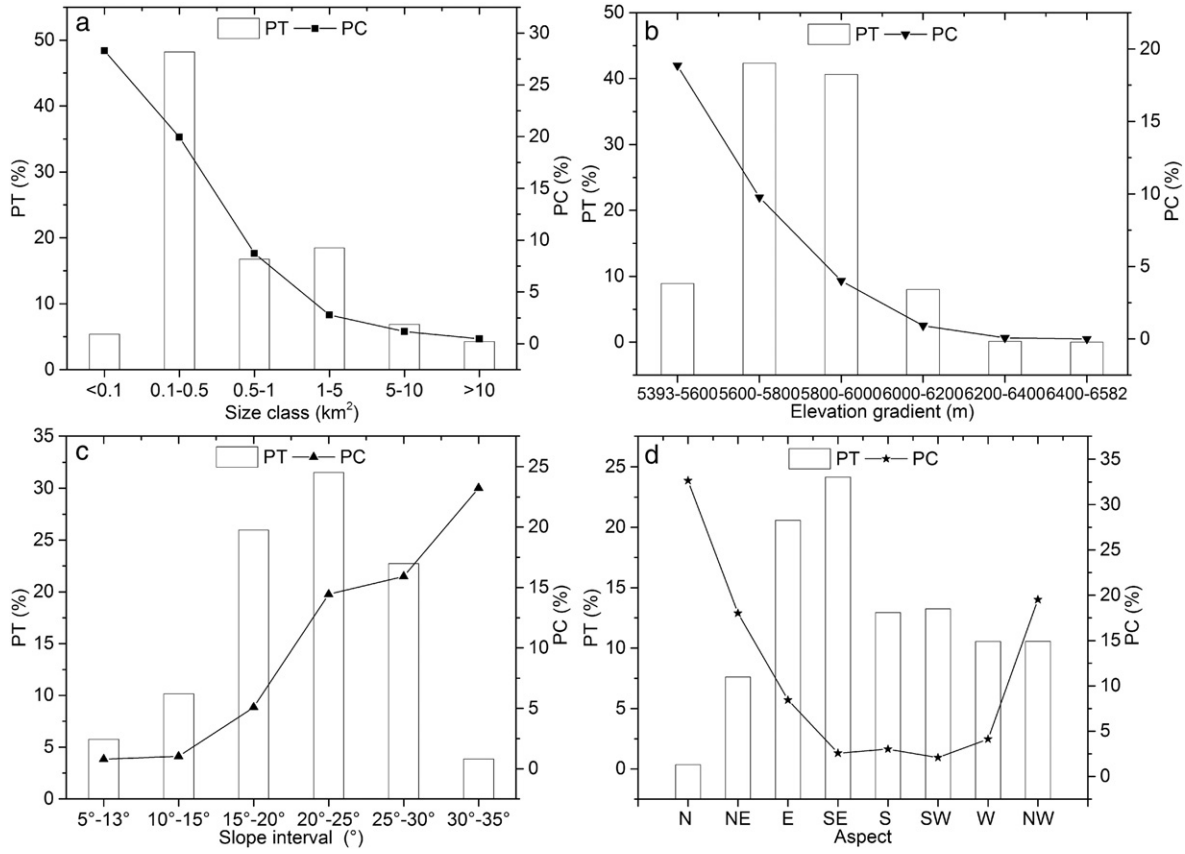

Fig. 6. Characteristics of glacier change from 1991 to 2013. (a) Decreases in the areal extent of glaciers as a function of size class. (b) Glacier area loss distribution vs. elevation interval. (c) Distribution of percentage glacial decreases as a function of slope. (d) Glacial area decreases as a function of aspect. PT correspond to glacier area changes of each classified group as a percentage of total area change and PC correspond to glacier area changes of each classified group as a percentage of glacier area distributed in corresponding group.

Conclusions

Landsat TM/ETM+, SRTM DEM v4.1, and Glas/ICESat remote sensing data of 303 glaciers in the Depuchangdake region show an increasing rate of glacial retreat between 1991 and 2013, during which time the glacier area decreased from 409 to 393 km^2. This decrease represents annual and total reductions in glacier area of 0.2 and 3.9%, respectively. The inverse relationship between area and rate of change indicates that small glaciers receded most rapidly. During the study period, the greatest glacial melting occurred for glaciers located between 5393 and 6000 m asl, with a reduction of 14.5 km^2, which amounts to 91.9% of the total glacial retreat in the study area. In addition, slope and aspect were also found to impact on the degree of glacier loss, with 90.4% of the total area loss occurring on slopes of 10–30°, and east- or southeasterly facing glaciers accounting for 44.3% of the total loss area. The mean glacier thinning rate was -0.40 ± 0.16 m w.e./yr,

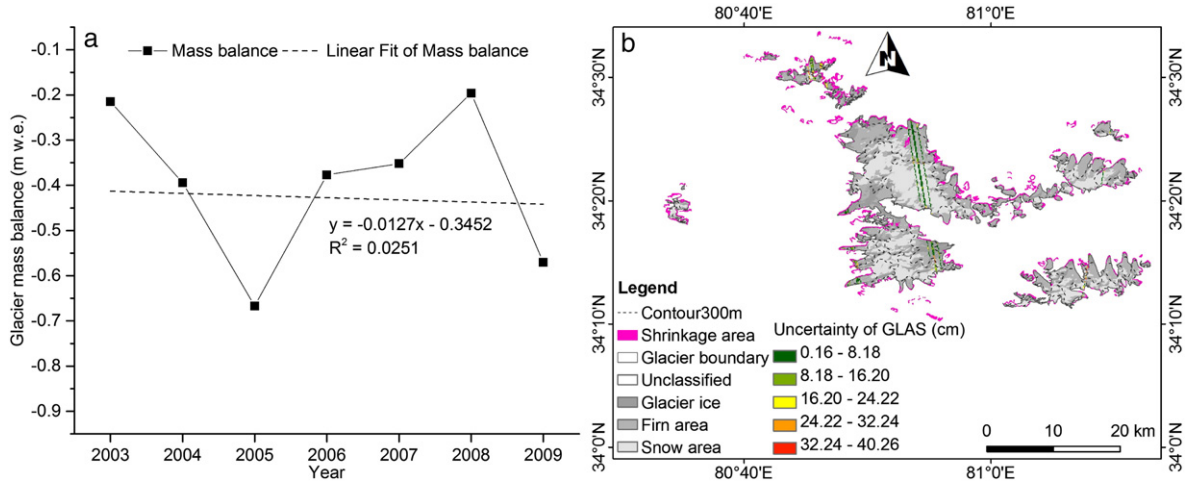

Fig. 7. Glacial mass loss changes estimated by Geoscience Laser Altimeter System (GLAS) elevation data and SRTM DEM in the Depuchangdake region. (a) GLAS-estimated glacial mass balance trends from 2003 to 2009 calculated from glacier volume loss. (b) Glacier material classifications (i.e., glacier ice, firn area and snow), glacier retreat areas between 1991 and 2013, and uncertainty in GLAS data. The distribution of interannual glacier covered area surface change was subdivided into 300 m intervals and estimated from GLAS footprint elevation data from 2003 to 2009.

https://doi.org/10.1016/j.yqres.2015.12.005 Published online by Cambridge University Press

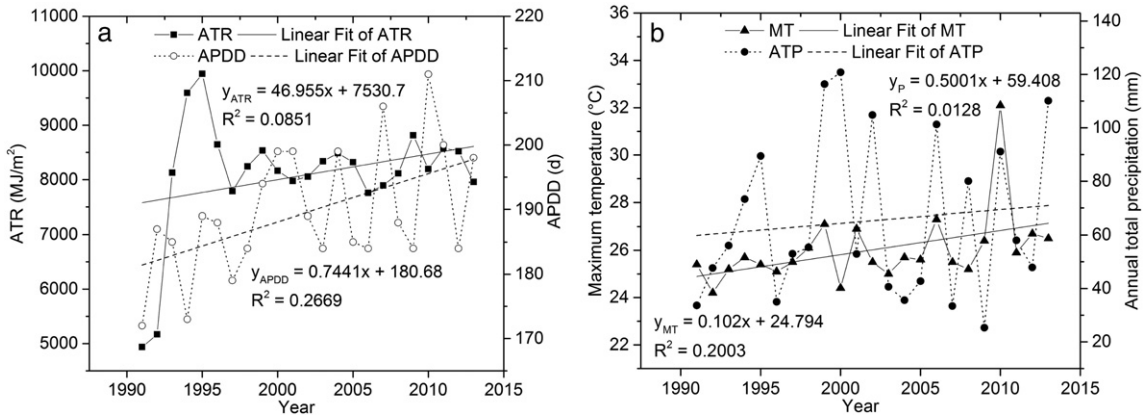

Fig. 8. Variations in the annual total radiation, annual positive degree days, maximum temperature, and precipitation at the Shiquanhe station from 1991 to 2013. ATT and APDD correspond to annual total radiation and annual positive degree days, respectively. MT and ATP correspond to maximum temperature and precipitation, respectively.

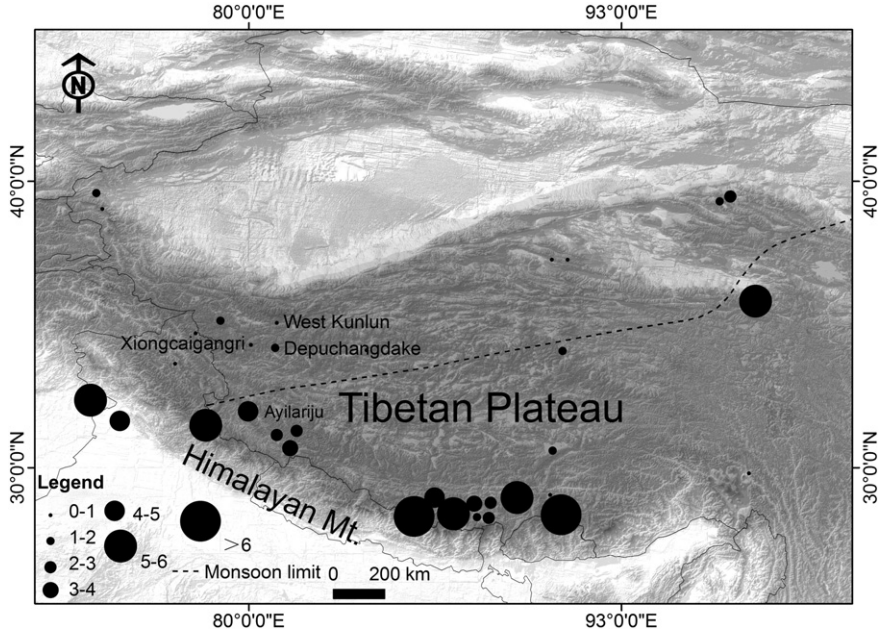

Fig. 9. Glacier area retreat rates in the Tibetan Plateau and bordering mountains (TPB; Units: % and $(10a)^{-1}$, modified from Li et al. (2015a).

equating to a glacier mass balance of -0.16 ± 0.07 km^3 w.e./yr. The total mass loss over the period 2003–2009 was -1.12 ± 0.45 km^3, with glacial meltwater flows into Jiezechaka, Woerba, Longmu and Lumajiangdong lakes of 0.38 ± 0.15, 0.07 ± 0.03, 0.28 ± 0.11 and 0.41 ± 0.16 km^3, respectively.

Climate data suggest that annual total radiation, annual positive degree days, and maximum temperature have been the main factors leading to glacier retreat, and although precipitation increased during the study period, it was insufficient to replenish the glaciers' mass loss.

Long-term observations, including high-resolution remote-sensing data, meteorological station data from different elevations within the glacier-covered area, and more ground-based observations are needed to gain a fuller understanding of glacier change in this region, and in particular to determine the differences between glaciers on eastern- and western-facing slopes. Furthermore, continuous monitoring of glacier changes would provide critical information for understanding the links between glaciers and climate change, which would greatly improve our ability to estimate the impact of glacier change on local water resources and lakes.

Table 4
Comparison of glacier retreat in Depuchangdake and nearby regions (*stands for estimated value).

Mountain name	Location	Period (a)	Rate (%/decade)	Average area (km^2)	Mean elevation (m)	Source
Xiongcaigangri	South Karakorum	1968–2013	0.3	1.18	6054.4	Li et al. (2015a)
Ayilariju	North Himalayas	1980–2011	4.7	0.68	5826.2	Li et al. (2015b)
West Kunlun	West Kunlun	1991–2011	0.3	4.85*	6028.2*	Li et al. (2013)
Depuchangdake	Transition zone	1991–2013	1.8	1.41	5962	This study

https://doi.org/10.1016/j.yqres.2015.12.005 Published online by Cambridge University Press

Acknowledgments

This work was supported by the National Natural Science Foundation of China (Grant Nos. 41101072, 41530748, 41025002 and 31100369). Landsat ETM/TM images, SRTM DEMs, and ICESat GLA S14 results were provided by the USGS. Meteorological data from the Shiquanhe station were kindly provided by the China Meteorological Data Sharing Service System.

Appendix A. Supplementary data

Supplementary data to this article can be found online at http://dx.doi.org/10.1016/j.yqres.2015.12.005.

References

Bajracharya, S.R., Maharjan, S.B., Shrestha, F., Guo, W., Liu, S.Y., Immerzeel, W., Shrestha, B., 2015. The glaciers of the Hindu Kush Himalayas: current status and observed changes from the 1980s to 2010. International Journal of Water Resources Development 31, 161–173.

Bolch, T., Kulkarni, A., Kääb, A., Huggel, C., Paul, F., Cogley, J.G., Frey, H., Kargel, J.S., Fujita, K., Scheel, M., Bajracharya, S., Stoffel, M., 2012. The state and fate of Himalayan glaciers. Science 336, 310–314.

Brahmbhatt, R.M., Bahuguna, I.M., Rathore, B.P., Singh, S.K., Rajawat, A.S., Shah, R.D., Kargel, J.S., 2015. Satellite monitoring of glaciers in the Karakoram from 1977 to 2013: an overall almost stable population of dynamic glaciers. The Cryosphere Discussions 9, 1555–1592.

Cao, B., Pan, B.T., Wang, J., Shangguan, D.H., Wen, Z.L., Qi, W.T., Cui, H., Lu, Y.Y., 2014. Changes in the glacier extent and surface elevation along the Ningchan and Shuiguan river source, eastern Qilian Mountains, China. Quaternary Research 81, 531–537.

Chen, F., Yu, Z., Yang, M., Ito, E., Wang, S., Madsen, D.B., Huang, X., Zhao, Y., Sato, T., John, B., Birks, H., Boomer, I., Chen, J., An, C., Wünnemann, B., 2008. Holocene moisture evolution in arid central Asia and its out-of-phase relationship with Asian monsoon history. Quaternary Science Reviews 27, 351–364.

Gardelle, J., Berthier, E., Arnaud, Y., Kääb, A., 2013. Region-wide glacier mass balances over the Pamir-Karakoram-Himalaya during 1999–2011. The Cryosphere 7, 1263–1286.

Gardner, A.S., Moholdt, G., Cogley, J.G., Wouters, B., Arendt, A.A., Wahr, J., Berthier, E., Hock, R., Pfeffer, W.T., Kaser, G., Ligtenberg, S.R.M., Bolch, T., Sharp, M.J., Hagen, J.O., van den Broeke, M.R., Paul, F., 2013. A reconciled estimate of glacier contributions to sea level rise: 2003 to 2009. Science 340, 852–857.

Ghosh, S., Pandey, A.C., Nathawat, M.S., Bahuguna, I.M., Ajai, 2014. Contrasting signals of glacier changes in Zanskar Valley, Jammu & Kashmir, India using remote sensing and GIS. Journal of the Indian Society of Remote Sensing 42, 817–827.

Hewitt, K., 2005. The Karakoram Anomaly? Glacier expansion and the 'elevation effect', Karakoram Himalaya. Mountain Research and Development 25, 332–340.

Immerzeel, W.W., van Beek, L.P.H., Bierkens, M.F.P., 2010. Climate change will affect the Asian water towers. Science 328, 1382–1385.

Kääb, A., Berthier, E., Nuth, C., Gardelle, J., Arnaud, Y., 2012. Contrasting patterns of early twenty-first-century glacier mass change in the Himalayas. Nature 488, 495–498.

Li, Z.G., Yao, T.D., Ye, Q.H., Tian, L.D., Li, C.C., 2011. Monitoring glacier variations based on remote sensing in the Luozha Region, Eastern Himalayas, 1980–2007. Geographical Research 26, 836–846 (in Chinese with English abstract).

Li, C.X., Yang, T.B., Tian, H.Z., 2013. Variation of West Kunlun Mountains glacier during 1990–2011. Progress in Physical Geography 32, 548–559 (in Chinese with English abstract).

Li, Z.G., Fang, H.Y., Tian, L.D., Dai, Y.F., Zong, J.B., 2015a. Changes in the glacier extent and surface elevation in Xiongcaigangri region, Southern Karakoram Mountains, China. Quaternary International 371, 67–75.

Li, Z.G., Tian, L.D., Fang, H.Y., Zhang, S.H., Zhang, J.J., Li, X.X., 2015b. Changes in glacier extent and surface elevations in the Ayilariju region, Western Himalayas, China. Environmental Earth Sciences (in press).

Ligtenberg, S.R.M., Helsen, M.M., van den Broeke, M.R., 2011. An improved semi-empirical model for the densification of Antarctic firn. The Cryosphere 5, 809–819.

Mir, R.A., Jainb, S.K., Sarafa, A.K., Goswamic, A., 2014. Glacier changes using satellite data and effect of climate in Tirungkhad basin located in western Himalaya. Geocarto International 29, 293–313.

Mölg, T., Maussion, F., Scherer, D., 2014. Mid-latitude westerlies as a driver of glacier variability in monsoonal High Asia. Nature Climate Change 4, 68–73.

Neckel, N., Kropáček, J., Bolch, T., Hochschild, V., 2014. Glacier mass changes on the Tibetan Plateau 2003–2009 derived from ICESat laser altimetry measurements. Environmental Research Letters 9, 014009.

Piao, S., Ciais, P., Huang, Y., Shen, Z.H., Peng, S.S., Li, J.S., Zhou, L.P., Liu, H.Y., Ma, Y.C., Ding, Y.H., Friedlingstein, P., Liu, C.Z., Tan, K., Yu, Y.Q., Zhang, T.Y., Fang, J.Y., 2010. The impacts of climate change on water resources and agriculture in China. Nature 467, 43–51.

Qiu, J., 2010. Measuring the meltdown. Nature 468, 141–142.

Raup, B.H., Kääb, A., Kargel, J.S., Bishop, M.P., Hamilton, G., Lee, E., Paul, F., Rau, F., Soltesz, D., Khalsa, S.J.S., Beedle, M., Helm, C., 2007. Remote sensing and GIS technology in the Global Land Ice Measurements from Space Project. Computers & Geosciences 33, 104–125.

Reuter, H.I., Nelson, A., Jarvis, A., 2007. An evaluation of void filling interpolation methods for SRTM data. International Journal of Geographical Information Science 21, 983–1008.

Shi, Y.F., 2008. Concise Glacier Inventory of China. Shanghai Popular Science Press, Shanghai.

Wang, L., Li, Z.Q., Wang, F.T., Edwards, R., 2014. Glacier shrinkage in the Ebinur lake basin, Tien Shan, China, during the past 40 years. Journal of Glaciology 60, 245–254.

Wang, W.C., Xiang, Y., Gao, Y., Lu, A.X., Yao, T.D., 2015a. Rapid expansion of glacial lakes caused by climate and glacier retreat in the Central Himalayas. Hydrological Processes 29, 859–874.

Wang, N.L., Wu, H.B., Wu, Y.W., Chen, A.A., 2015b. Variations of the glacier mass balance and lake water storage in the Tarim Basin, northwest China, over the period of 2003–2009 estimated by the ICESat-GLAS data. Environmental Earth Sciences 74, 1997–2008.

Wiltshire, A.J., et al., 2014. Climate change implications for the glaciers of the Hindu Kush, Karakoram and Himalayan region. The Cryosphere 8, 941–958.

Wu, H.B., Wang, N.L., Jiang, X., Guo, Z.M., 2014. Variations in water level and glacier mass balance in Nam Co lake, Nyainqentanglha range, Tibetan Plateau, based on ICESat data for 2003–09. Annals of Glaciology 55, 239–247.

Xiang, Y., Gao, Y., Yao, T.D., 2014. Glacier change in the Poiqu River basin inferred from Landsat data from 1975 to 2010. Quaternary International 349, 392–401.

Yang, K., Wu, H., Qin, J., Lin, C.G., Tang, W.J., Chen, Y.Y., 2014. Recent climate changes over the Tibetan Plateau and their impacts on energy and water cycle: a review. Global and Planetary Change 112, 79–91.

Yao, T.D., 2008. Map of Glaciers and Lakes on the Tibetan Plateau and the Surroundings. Xi'an Cartographic Publishing House.

Yao, T.D., 2010. Glacial fluctuations and its impacts on lakes in the southern Tibetan Plateau. Chinese Science Bulletin 55, 2071.

Yao, T.D., Thompson, L., Yang, W., Yu, W.Y., Gao, Y., Guo, X.J., Yang, X.X., Duan, K.Q., Zhao, H.B., Xu, B.Q., Pu, J.C., Lu, A.X., Xiang, Y., Kattel, D.B., Joswiak, D., 2012. Different glacier status with atmospheric circulations in Tibetan Plateau and surroundings. Nature Climate Change 2, 663–667.

Ye, Q.H., Kang, S.C., Chen, F., Wang, J.H., 2006. Monitoring glacier variations on Geladandong mountain, central Tibetan Plateau, from 1969 to 2002 using remote-sensing and GIS technologies. Journal of Glaciology 52, 537–545.

Ye, Q.H., Yao, T.D., Naruse, R., 2008. Glacier and lake variations in the Mapam Yumco basin, western Himalayas of the Tibetan Plateau, from 1974 to 2003 using remote sensing and GIS technologies. Journal of Glaciology 54, 933–935.

Zhang, Y.S., Yao, T.D., Pu, J.C., 1996. The characteristics of ablation on continental type glaciers in China. Journal of Glaciology and Geocryology 18, 147–154 (in Chinese with English abstract).